Journal of Applied Sciences

ISSN 1812-5654

science alert

ANSInet
an open access publisher
http://ansinet.com

Journal of Applied Sciences 12 (24): 2592-2597, 2012
ISSN 1812-5654 / DOI: 10.3923/jas.2012.2592.2597

Investigation of Starting Behaviour of a Free-piston Linear Generator

Ezrann Zharif Zainal Abidin, Abdulwehab A. Ibrahim, A. Rashid A. Aziz and Saiful A. Zulkifli
Center for Automotive Research and Electric Mobility, Department of Mechanical Engineering,
Universiti Teknologi PETRONAS, Bandar Seri Iskandar, 31750 Tronoh, Perak, Malaysia

Abstract: A linear engine coupled to a permanent-magnet assembly becomes a linear generator engine (LG) which can produce electrical power. Its working principle is based on the free-piston two-stroke engine. The main difference between the LG and a conventional crank-slider engine is that the LG has only one moving part which is the piston-rod assembly (translator). The piston-rod assembly consists of two pistons and a rod, with one piston connected to each end of the rod and a magnet assembly at the center of the rod. Combustion energy will cause the piston-rod assembly to move freely back and forth between the two engine blocks. Magnetic field from the permanent magnet assembly will cut through conductor coils-which are externally located within the stationary part of the LG (stator iron)-to generate electricity. Thus, electrical power is generated directly from the moving piston. For starting of the generator, the LG is operated in a reverse process-as a motor, whereby current is injected into the coils to produce force to reciprocate the translator against the forces of compression of the engine blocks, in order to produce combustion. Experimental work described in this paper shows promising results on combustion pressure using an upgraded MOSFET inverter and gate driver. Previous work managed to produce only 9 bar of peak combustion pressure during starting, using 5 sets of standard automotive lead-acid batteries. With the upgraded system and further engine optimization, the LG managed to produce 12.7 bar of combustion pressure and a highest IMEP of 0.8 bar. This paper presents results of the newly installed drivers and optimization of the combustion process to achieve higher combustion pressure.

Key words: Linear generator, IMEP, cylinder pressure, MOSFET, gate driver; equivalence ratio

INTRODUCTION

A linear generator engine (Fig. 1) is based on a free-piston engine where it freely moves without any mechanical part relating to its motion. It is a crank-less reciprocating engine, having no connections to any camshaft, compressor or power-steering pump; thus, it has no mechanical output and experiences less friction. Due to the absence of the crankshaft, its side load friction from the piston is reduced. As a result, the LG has a high mechanical efficiency. It's simple design contains fewer parts, is less costly, less maintenance is required and is more reliable. Due to its small compact design, it has a high power to weight ratio (Zulkifli, 2007; Zulkifli *et al*., 2009). The objectives of this research are to integrate and to test the new MOSFET inverter and gate driver to the current system and to be able to motor the LG from 3 batteries up to 7 batteries and to perform combustion while motoring with 3 and 5 batteries.

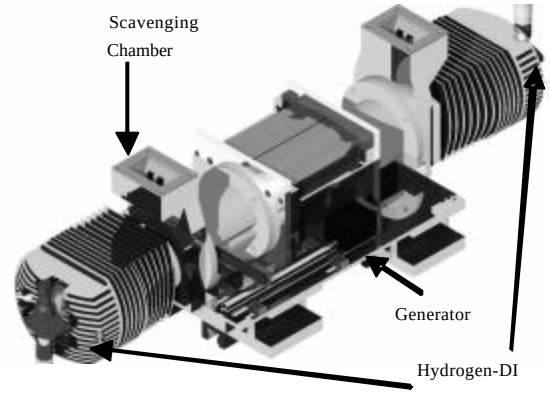

Fig. 1: UTP two-stroke hydrogen-DI linear generator free-piston engine prototype

LINEAR GENERATOR

Working principle: The LG's basic operating principle is based on a 2-stroke engine where exhaust and intake stroke is completed within 1 cycle and the compression and power stroke is 1 cycle. The difference between 2-stroke and 4-stroke engine is that a 4-stroke engine produces 1 power stroke in every 2 revolutions, while a

Corresponding Author: Ezrann Zharif Zainal Abidin, Center for Automotive Research and Electric Mobility, Department of Mechanical Engineering,Universiti Teknologi PETRONAS, Bandar Seri Iskandar, 31750 Tronoh, Perak, Malaysia

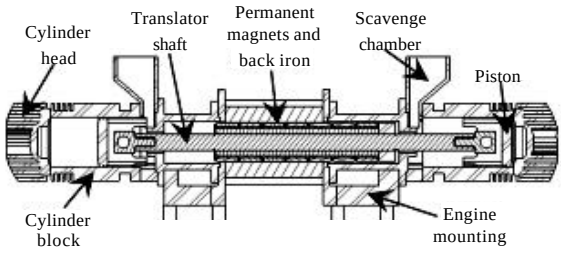

Fig. 2: LG cross-sectional view

2-stroke engine produces 1 power stroke in each revolution. The LG is operated as a motor for starting of the LG. During motoring, air will enter through the opening ports into the combustion chamber. Towards the end of the compression process, hydrogen is injected directly into the combustion chamber as a fuel to combust by the spark plug. The combustion energy will then push the piston towards the other end and the process repeats itself. The back and forth motion of the translator (which consists of a permanent magnet assembly as shown in Fig. 2 will cut the magnetic fields to produce electricity (Hanipah, 2008).

This output energy can then be used to charge batteries or directly power an electric motor in a series configuration of a Hybrid Electric Vehicle (HEV). As for lubrication, it uses the same concept as most 2-stroke engines: lubrication is injected into the incoming air going into the cylinder in the form of fine mist. Once it is in contact with the surface, the lubrication provides smooth movement of mechanical parts such as the shaft and piston (Ibrahim *et al*., 2011).

Technical review of hydrogen-fueled internal combustion engine: This study discusses combustion characteristics, problems, future development and optimization of a hydrogen internal combustion engine (H_2ICE) to achieve better performance and near zero emission. Due to the characteristics of hydrogen, H_2ICE is able to burn cleanly and work efficiently at ultra-lean combustion and low engine load while reducing the production of NO_x. It is said that the main problem with using hydrogen is the pre-ignition (since hydrogen has a low ignition energy) which is caused by engine hot spots, such as spark electrodes, valves or engine deposits which can cause engine peak power output to be reduced by 50% compared to engine operation with gasoline (White *et al*., 2006).

Therefore, for practical application, the maximum Equivalence Ratio (ER) and consequently, peak power output can be limited by the pre-ignition limit. This problem can be minimized using cold-rated spark plugs, low coolant temperature, optimized fuel-injection timing and advanced engine control strategies such as intake charge cooling, variable valve timing for effective scavenging of exhaust residuals, advanced ignition systems and hydrogen Direct Injection (DI) (White *et al*., 2006).

The direct injection H_2ICE has long been viewed as one of the most attractive advanced H_2ICE options since it produces higher volumetric efficiency due to the ability to inject the fuel after the intake valve is closed. This method also has a good potential to avoid pre-ignition. It is known that the potential of DI-H_2ICE power density to be approximately 115% that of an identical engine operated on gasoline. The challenge with DI-H_2ICE is that in-cylinder injection requires hydrogen-air mixing in a very short time. Experimental evidence demonstrates that complete mixing in an engine takes approximately 10 msec (White *et al*., 2006).

Another interesting fact is that if the H_2ICE is used to drive an alternator that generates electricity, it can be operated and optimized for single-speed operation at maximum power (White *et al*., 2006).

Performance characteristics of a hydrogen-fuelled free-piston internal combustion engine and linear generator system: This study describes the performance of a Free-piston Engine (FPE) with an engine capacity of 150.8 or 100.5 cc depending on 2 types of fuel applications: either Compressed Natural Gas (CNG) or hydrogen. When CNG fuel is used, the piston stroke is elongated for half of the original stroke to draw more useful work out of the generator (Woo *et al*., 2009). The engine speed is controlled mainly by adjusting the ignition timing.

From experimental data shown in Woo *et al*. (2009), the peak cylinder pressure with combustion using CNG as fuel is around 25-30 bar with piston frequency of 13 Hz and a few recorded misfires. With hydrogen as fuel, the test engine was operated at 13 Hz with peak cylinder pressure of 30-35 bar. The increase in pressure when using hydrogen is due to the high combustion speed of hydrogen. From the rate of heat release graph, the combustion duration is longer for CNG compared to hydrogen. All the combustion heat released recorded is before the piston's TDC. Ignition timing was adjusted to adjust the position of the peak cylinder pressure to occur after TDC but due to instability of the engine, it stops after several minutes of operation.

APPROACH AND METHODS

Experimental setup: A control and data acquisition (DAQ) system based on National Instruments (NI)

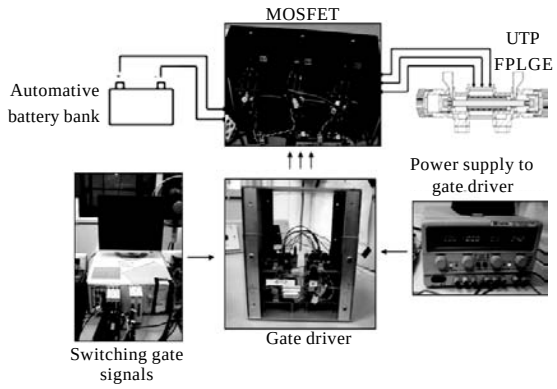

Fig. 3: Experimental setup for linear generator

hardware and software is used to control the engine and to log data during experimentation (Fig. 3). Data logging is performed on a 10-kHz sampling frequency to attain accurate results for data post-processing. For current injection and switching purposes, signal from the control system is amplified by the gate driver to operate the MOSFET inverter. The battery bank consists of 7 sets of 12 V automotive lead-acid batteries connected in series, to provide electrical energy to the LG during the motoring and starting process.

For the combustion experiments, hydrogen gas is used as the fuel. It is directly injected into the combustion chamber and ignited by spark plugs. The injection and ignition timing are all controlled by the NI control and DAQ system, running LabVIEW 7.1 software.

RESULTS AND DISCUSSION

Previously, an inverter based on IGBT (insulated-gate bipolar transistors) was used as the main driver for LG since it can handle far greater voltage and current levels compared to a MOSFET inverter (Ibrahim *et al*., 2011). Yet, due to its complexity of operation and based on previous experimental results which were not very encouraging, it was then agreed to perform further testing using MOSFETs but with an upgraded gate driver. New MOSFET transistors from International Rectifier (part No. IRFB4110PBF) are selected to be able to handle up to 100 Volts and 160 Amps (total of 8 batteries) of operation. Also, a new gate driver is used to operate it.

Using the new MOSFET transistors: Motoring comparison between new and old gate drivers: Installation of a new MOSFET gate driver takes place to replace the old and problematic gate driver which had been causing unstable engine operations. Testing is performed to

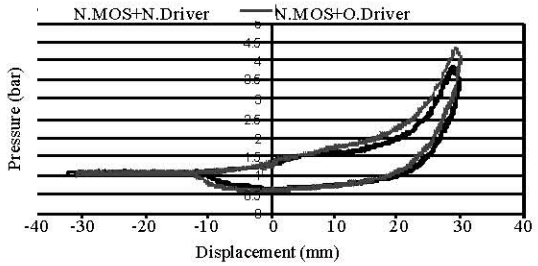

Fig. 4: Pressure vs. displacement for motoring with 3 batteries

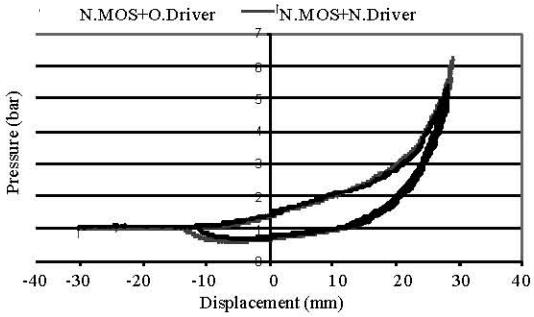

Fig. 5: Pressure vs. displacement for motoring with 5 batteries

compare motoring results with the previous MOSFET gate driver and to continue with further experiments. Figure 4 below compares between the new and old gate drivers in motoring tests with 3 batteries. The old driver produces a higher peak cylinder pressure of 4.2 bar while the new gate driver produces only 3.87 bar.

The new gate driver has a lower pressure due to slightly lower battery power (36 volts) while fully charged battery is at 38 volts. A 2-volt difference is still acceptable to proceed with experiments but it will produce less compression pressure. The important aspect is that both graphs show similar movement and pressure patterns.

Figure 5 shows results of motoring with 5 batteries. As before, the slightly less battery voltage with the new gate driver produces a lower peak cylinder pressure of 5.5 bar, compared to 6.98 bar with the new gate driver. Otherwise, the trend in both movement and pressure profiles is the same. These results conclude that the new gate driver is stable and reliable for further experimentation.

Motoring with the new MOSFET transistors and gate drivers: using 3, 5, 6 and 7 batteries: With the new MOSFET inverter and gate driver installed, further experiments can be performed since it can handle higher

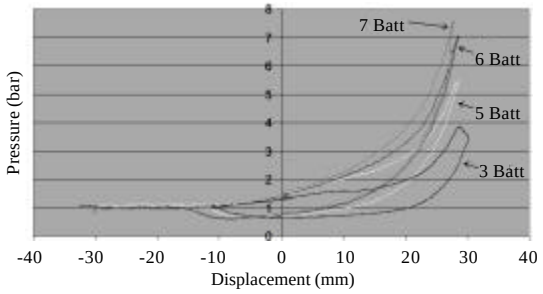

Fig. 6: Pressure profiles of motoring from 3 to 7 batteries

Table 1: Experimental results of motoring from 3 to 7 batteries

No. of batteries	3	5	6	7
Peak pressure (bar)	3.85	5.43	7	7.58
Top velocity (m sec^{-1})	0.5	1.1	1.5	2

voltage and current of using more batteries. Motoring is carried out using 3, 5, 6 and 7 batteries which correspond to 36, 60, 72 and 80 V, respectively. From Fig. 6, it can be seen that with higher motoring voltage, peak pressure will increase and the pressure profiles become steeper (move closer towards the y-axis). Thus, motoring with 7 batteries achieves higher compression pressure faster and at shorter stroke compared to 3, 5 and 6 batteries. The comparison of pressure and velocity is shown in Table 1.

Previously it can be seen (Fig. 7) that motoring with 7 batteries produces a higher compression pressure on a shorter stroke. This is because with higher voltage, piston speed is higher, resulting in less air leakage through the piston rings, thus producing higher compression pressure. Having higher compression pressure will produce a denser air charge for combustion. To compare the velocities, 7-battery motoring has the highest piston speed of 2 m sec^{-1}, followed by 6 batteries (1.5 m sec^{-1}), 5 batteries (1.1 m sec^{-1}) and 3 batteries (0.5 m sec^{-1}).

Motoring with 3 batteries, with combustion: Many combustion cycles have been experimented using 3 batteries and the highest combustion pressure that could be obtained was 9.4 bar with the following settings: injection at 27 mm, 1.6 Equivalence Ratio (ER), ignition at 28.125 mm and TDC at 28.125 mm. Injection points are varied from 17 to 27 mm and the resultant PV diagrams are shown in Fig. 8.

Moving the injection point closer to TDC results in higher combustion pressure. Injection at 17 mm is a little too early and due to the slow piston speed in motoring with 3 batteries, considerable charge leaks through the piston rings causing low combustion pressure. Since injection points nearer to TDC will produce higher pressure, further attempt to experiment with 17 mm injection is halted.

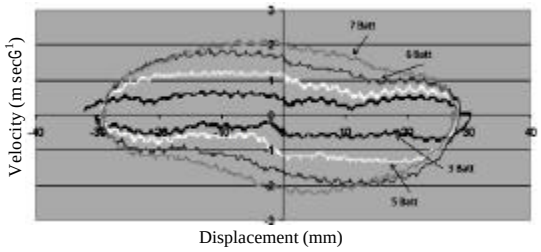

Fig. 7: Velocity profiles of motoring from 3 to 7 batteries

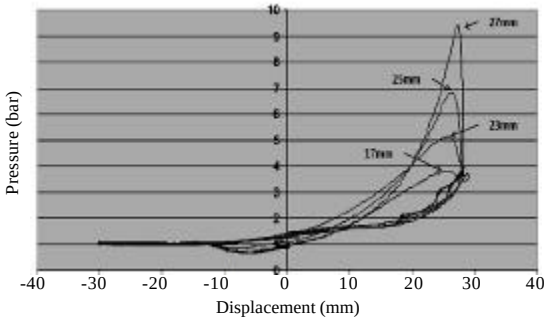

Fig. 8: Pressure vs. displacement with constant fuel ER of 1.6

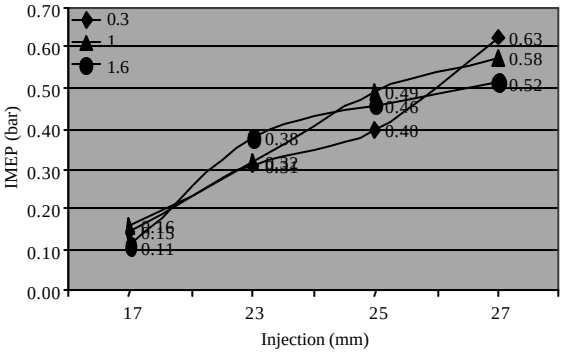

Fig. 9: IMEP vs. injection point with varied fuel ER of 0.3, 1 and 1.6

In Fig. 9 IMEP is determined and plotted for different values of ER, while the injection point is varied, to show overall engine performance. It can be seen that the relation of IMEP to injection point approximates a linear trend. Late injection at 27 mm produces better IMEP. The highest IMEP is produced by 27 mm injection with 0.3 ER which is at 0.63 bar. The reason a higher ER produces slightly lower IMEP at 27 mm injection will be discussed in the following section.

Motoring with 5 batteries, with combustion (varying injection point and equivalence ratio): Injection point is

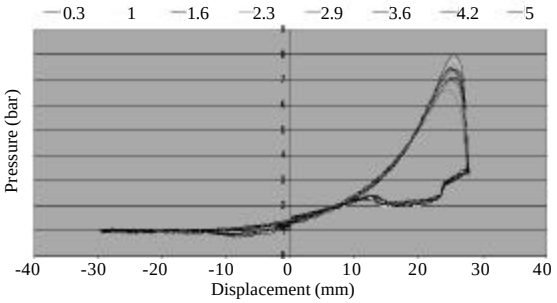

Fig. 10: Pressure vs. displacement for constant injection point of 23 mm

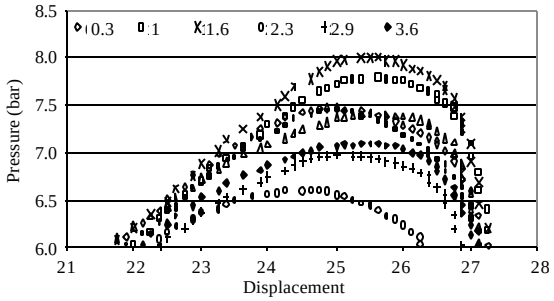

Fig. 11: Pressure vs. displacement for constant injection point of 23 mm (close-up)

selected at several points: early injection (23 mm), middle injection (25 mm) and late injection (27 mm). For each constant injection point, hydrogen fuel is varied with Equivalence Ratio (ER) of 0.3 to 5. LG is motored using 5 batteries, with the Top Dead Center (TDC) at 28 mm and ignition point at 27.625 mm.

Varying fuel ER with fixed injection point of 23 mm: Figure 10 shows the PV diagram for motoring runs with a fixed 23 mm injection point and varied fuel ER. In terms of trend, the overall fuel range produces the same combustion behaviour but at 1 and 1.6 equivalence ratio, higher combustion pressure is produced (7.8 and 8 bar, respectively). Figure 11 shows a close-up view of the peaks of the pressure curves, for a clearer comparison.

The highest pressure recorded in Fig. 11 is 8 bar with an ER of 1.6 while the lowest is 6.6 bar at 2.3 ER. It is noticed that there is not much pressure difference between ER of 2.9 to 5 (pressure range is 7 to 7.4 bar). This indicates better combustion pressure at ER stoichiometric of 1 and slightly rich ER of 1.6.

Varying fuel ER with fixed injection point of 25 mm: Figure 12 shows a close-up of the PV diagrams of motoring with an injection point of 25 mm. The highest pressure values recorded are 10.6 and 10.5 bar for fuel ER of 1.6 and 1, respectively. The rest of ER only produces combustion pressure in the range of 8.9 to 9.1 bar. Combustion pressure produced by injecting fuel at 25 mm seems to perform better compared to 23 mm.

Varying fuel ER with fixed injection point of 27 mm: Injection point at 27 mm is very near to the ignition point of 27.625 mm. Results are shown in Fig. 13. Comparing the 3 injection points (23, 25 and 27 mm), the highest combustion pressure recorded is 12.7 bar at 27 mm injection with 1 ER, followed by 1.6 ER (12 bar) and 0.3 ER (11.78 bar).

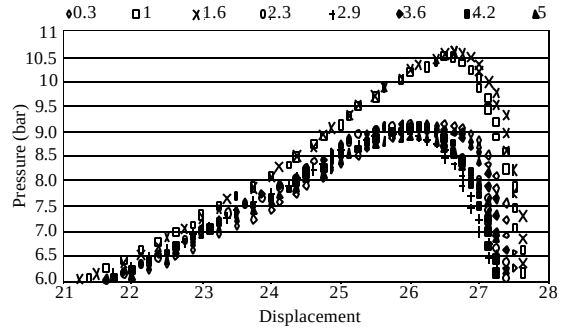

Fig. 12: Pressure vs. displacement for constant injection point of 25 mm (close-up)

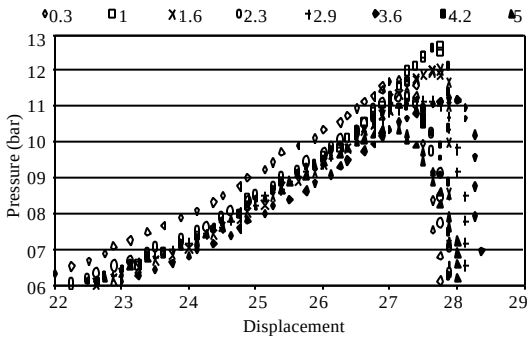

Fig. 13: Pressure vs. displacement for constant injection point of 27 mm (close-up)

It seems that high combustion pressure is frequently produced at near stoichiometric point which is at 1 ER and slightly rich mixture at 1.6 ER. This is also true in previous studies (Hanipah, 2008). Fuel with higher than 1.6 ER would lower the chance of complete combustion due to lack of air as reactant in the cylinder.

Varying injection point with constant fuel ER: To clearly show the effect of varying the injection point, a constant fuel of 1 ER is chosen since it produces the highest

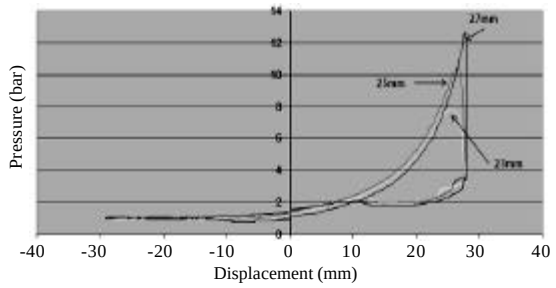

Fig. 14: Pressure vs. displacement for constant fuel of 1 ER

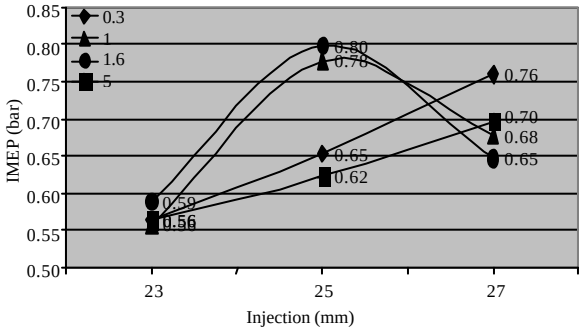

Fig. 15: IMEP vs. injection point with fuel ER of 0.3, 1, 1.6 and 5

combustion pressure across the range of injection points experimented previously: 12.7 bar. A comparison graph is plotted in Fig. 14.

It can be clearly seen that when fuel injection is near to the ignition point and TDC, higher overall combustion pressure are produced throughout the ER range. This is because late injection improves volumetric efficiency, resulting in higher compression pressures (denser charge) prior to ignition (Hanipah, 2008).

Indicated mean effective pressure (IMEP): IMEP is a useful relative measurement of engine performance; hence, Fig. 15 is plotted for fuel ER of 0.3, 1, 1.6 and 5-chosen to compare overall engine performance since it varies from lean to rich. Highest IMEP obtained is 0.8 bar produced by 1.6 ER at 25 mm injection, followed by 0.78 bar (1 ER, 25 mm injection) and 0.76 bar (0.3 ER, 27 mm injection). The reason highest IMEP is produced with 25 mm injection point is because the charge has sufficient time to mix fuel and air before combusting at the 27.625 mm ignition point. The duration of time between injection event (25 mm) and ignition event (27.625 mm) is 12.7 msec, allowing for a complete air-fuel mixing (White *et al*., 2006).

CONCLUSION

It can be concluded that late injection will produce higher combustion pressure but due to insufficient time for air-fuel mixing, IMEP would be affected. Lower battery capacity (3 batteries) produces lower combustion pressure due to the lower compression pressure, thus failing to deliver denser air charge at the point before ignition. The most effective range of combustion occurs with a fuel ER of 1 and 1.6. Hence, combustion with 1.6 ER at 25 mm injection-producing an IMEP of 0.8 bar-is favorable. Motoring with 5 batteries, using the new MOSFET transistors and new gate driver, looks very promising for starting and combustion of the LG. Further experimentation of the LG will be focused on combustion with higher battery capacity to produce higher combustion pressure and higher IMEP to achieve stable idling.

REFERENCES

Hanipah, M.R., 2008. Combustion process in a two-stroke, H2-DI linear generator free-piston engine during starting. M.Sc. Thesis, Universiti Teknologi PETRONAS, Bandar Sri Iskandar, Malaysia.

Ibrahim, A.A., A.R.A. Aziz, E.Z.Z. Abidin and S.A. Zulkifli, 2011. The operation of free piston linear generator engine using MOSFET and IGBT drivers. J. Applied Sci., 11: 1791-1796.

White, C.M., R.R. Steeper and A.E. Lutz, 2006. The hydrogen-fueled internal combustion engine: A technical review. Int. J. Hydrogen Energy, 31: 1292-1305.

Woo, Y., Y. Lee and Y. Lee, 2009. The performance characteristics of a hydrogen-fuelled free piston internal combustion engine and linear generator system. Int. J. Low-Carbon Tech., 4: 36-41.

Zulkifli, S.A., 2007. Modeling, simulation and implementation of rectangular commutation for starting of free-piston linear generator. M.Sc. Thesis, Universiti Teknologi Petronas, Malaysia.

Zulkifli, S.A., M.N. Karsiti and A.R. A-Aziz, 2009. Investigation of linear generator starting modes by mechanical resonance and rectangular current commutation. Proceedings of the IEEE International Electric Machines and Drives Conference, May 3-6, 2009, Miami, FL., pp: 425-433.